Multiple devil's staircase and type-V intermittency

Shi-Xian Qu,[1] Shunguang Wu,[2] and Da-Ren He[3,4,5,*]
[1]*Department of Basic Courses, Xian Petroleum Institute, Xian 710065, China*
[2]*Department of Physics, Northwestern University, Xian 710069, China*
[3]*CCAST (World Laboratory), P.O. Box 8730, Beijing 100080, China*
[4]*Department of Physics, Teachers College, Yangzhou University, Yangzhou 225002, China*
[5]*Institute of Theoretical Physics, Academia Sinica, Beijing 100080, China*
(Received 5 November 1996; revised manuscript received 10 October 1997)

We have observed a ''multiple devil's staircase'' in a one-dimensional (1D) map including two discontinuous regions. Both end points of each phase-locked plateau in the staircase are confined by the conditions of collision between the periodic orbit and one of the discontinuous region edges. There are more modes of the collision than in a 1D map including only one discontinuous region. This complexity makes the whole staircase lose monotonicity, self-similarity, and the ''Farey tree rule'' for a description of the plateau length distribution. However, the staircase consists of many conventional complete devil's staircases, many of them having their own threshold of transfer to chaos via a type-V intermittency. Therefore the parameter space can be divided into three parts. In the first part only periodic attractors appear. In the second part periodic and chaotic attractors appear alternatively, and the system displays type-V intermittency frequently. In the last part only chaotic attractors exist. [S1063-651X(98)10601-3]

PACS number(s): 05.45.+b

I. INTRODUCTION

Recently, there has been considerable interest in piecewise smooth maps. These maps may describe some practical systems, such as relaxation [1–15] or impact [16–22] oscillators, and display some dynamic phenomena different from what can be observed in a everywhere-differentiable map [1–22]. One of these phenomena is a new type of intermittency, named type-V intermittency [10–15], that happens via a collision of a periodic point with a discontinuous or nondifferentiable point of the map. This type of intermittency shows a logarithmic dependence of the average laminar length on the control parameter ϵ [10,11], a hyperbolic secant invariant distribution of the laminar lengths [13], and a $1/\ln\epsilon$ dependence of the Lyapunov exponent [15,16]. In different practical fields, three research groups have published experimental proofs of type-V intermittency [12,23,24].

When studying the scaling behavior of the Lyapunov exponent in type-V intermittency, Lamba and Budd [16] showed that in a discontinuous one-dimensional map a sequence of periodic attractors should appear before the system transfers to a chaotic motion via a type-V intermittency. For this conclusion, Wu, Ding, and He [15] presented evidence in a piecewise linear model. They also found that in the model the periodic attractors emerging before type-V intermittency form a ''conventional complete devil's staircase (CCDS).'' This concept will be discussed here.

The devil's staircase is a structure describing phase locking behavior in quite different contexts [25], such as a one-dimensional Ising model with long-range interactions [26], the Frenkel-Kontorowa model of atoms adsorbed on a periodic substrate [27], the three-dimensional Ising model with competing interactions [28], the current-driven Josephson junction [29], the driven electrical conductivity of barium sodium niobate crystals [30], driven charge-density-wave systems [31], and driven electronic relaxation oscillators [32]. This kind of dynamics can be described by one-dimensional discrete maps of the circle onto itself, the so-called ''circle maps.'' In such a map a winding number ω can be defined as the mean number of rotations per iteration. When the control parameter ϵ is varied, the function $\omega(\epsilon)$ is locked onto every single rational value to form a devil's staircase in the ϵ-ω plane [25,33]. The staircases often become complete on an one-dimensional set in the parameter space separating different kinds of dynamics. The complementary set to a complete staircase is a Cantor set of fractal dimension $D \leqslant 1$ [33].

To our knowledge, all the observed complete devil's staircases have three common characteristics. We shall use the term CCDS to denote them. First, the winding number, ω, is always locked to a rational in a nonzero interval $\Delta\epsilon$. Second, the rule of the distribution of $\Delta\epsilon$ lengths can be fully described by a Farey tree. That means if there are two winding numbers, $\omega = M/s$ and $\omega' = M'/s'$ (M and s are integers), which are phase locked in $\Delta\epsilon$ and $\Delta\epsilon'$, then the winding number of the largest phase-locking interval (or say phase-locked plateau) between $\Delta\epsilon$ and $\Delta\epsilon'$ is $(M+M')/(s+s')$. In the following we shall call this rule the ''Farey tree rule.'' Last, the whole staircase $\omega(\epsilon)$ shows monotonicity and exact self-similarity. This is exactly what Wu, Ding, and He reported in Ref. [15].

The mapping function studied in Ref. [15] actually has two gaps (two discontinuous regions). As shown in Fig. 1, there is a gap between points D and E, and another gap between points A and F. Gap DE plays a very important role in the creation of the CCDS. Each phase-locked plateau in the CCDS vanishes when ϵ reaches a threshold at which the

*Author for correspondence. Address correspondence to Department of Physics, Teachers College, Yangzhou University, Yangzhou 225002, China.

 © 1998 The American Physical Society

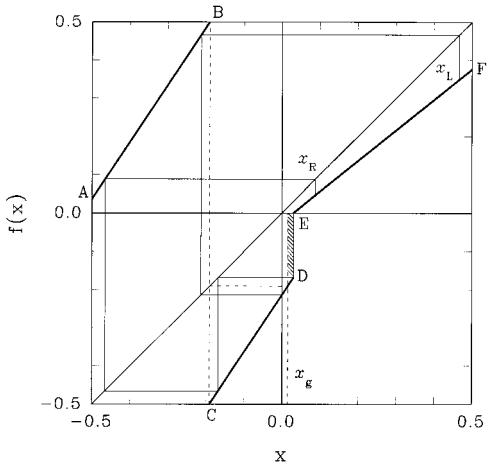

FIG. 1. A schematic drawing of mapping function (1). The wider solid lines show the mapping function. As shown by the dashed lines, the second backward images of x_F and x_A fall together at the center of the exit of the channel that is indicated by $x_g = f^{-2}(x_F) = f^{-2}(x_A)$. The thin solid lines starting from point E shows the iteration trajectory escaping from the right end point of the exit of the channel. It is reinjected into the channel at x_R. The thin solid lines starting from point (0,0) shows the trajectory from the left end point of the exit. It is reinjected into the channel at x_L.

periodic orbit collides with either of the gap edges. At the left end point of the plateau, ϵ_L, the periodic orbit collides with point D, while at the right end point of the plateau, ϵ_R, it collides with E. After the collision the winding number is locked in another rational. In the system studied in Ref. [15], the role of gap AF is unimportant, because the mapping function was constructed so that the iteration always visits segment CD twice and AB once. The reinjection behavior does not change significantly when the iteration out of the exit of the channel passes the ''implicit discontinuous point'' $x_g = f^{-2}(x_A) = f^{-2}(x_F)$. We say that the reinjection mechanism is ''simple'' in this case. This simplicity induces a simple CCDS.

What will happen if the mapping function is changed so that the reinjection behavior becomes significantly different when the iteration passes x_g? In that case gap AF will play an important role in the creation of the staircase as well, and the complexity of the reinjection mechanism will show its influence on the structure of the staircase. The new characteristics of the staircase should be an interesting feature of a ''multigap'' map. This is what we want to discuss in this paper. In Sec. II of this paper we shall describe the modified system. In Sec. III we shall derive the mathematical expression of the new staircase. In Sec. IV we shall report the characteristics of type-V intermittency in this system. In Sec. V a discussion of some further questions will be presented.

II. THE SYSTEM

The mapping function, which can be viewed as a simplified model of an electronic relaxation oscillator [11] and which was discussed in Ref. [15], is modified so that the reinjection mechanism becomes ''complicated,'' as shown in Fig. 1. The map reads:

$$f(x) = \begin{cases} f_{11}(x) = k_1 x + b_{11}, & x \in [-0.5, x_B] \\ f_{12}(x) = k_1 x + b_{12}, & x \in (x_B, \epsilon) \\ f_2(x) = k_2 x + b_2, & x \in [\epsilon, 0.5], \end{cases} \quad [\text{mod}1] \quad (1)$$

where k_2 should be little bit smaller than unity so as to form a specific channel in type-V intermittency [11,15]. k_1 should be quite larger than unity, so that the system's behavior can be chaotic. Our study shows that the dynamics of the system is qualitatively the same when k_2 or k_1 changes in this range. Here we choose $k_1 = 1.5$, $b_{11} = (2k_1 + 1 - k_1^2\epsilon)/2(k_1 + 1)$, $b_{12} = -(1 + k_1^2\epsilon)/2(k_1 + 1)$, $k_2 = 0.8$, and $b_2 = -k_2\epsilon$. The parameter ϵ denotes the horizontal coordinate of point E, the width of the exit of the channel, and is chosen as the control parameter. It is useful to note that $y_E \equiv 0$, x_B can be expressed as $x_B = 0.5k_1\epsilon + b_{12}$, and $y_A = x_E = \epsilon$, and $y_D = k_1\epsilon + b_{12}$. We define b_{11}, b_{12}, and b_2 as functions of k_1, k_2, and ϵ instead of being constants in order to keep x_g, the second backward image of both x_A and x_F, always in the middle of the exit of the channel, i.e., $x_g = \epsilon/2$, and let the reinjection behaviors become qualitatively different when an iteration out of the channel passes x_g. One will see that it is very important for the appearance of the specific devil's staircase in this system.

Actually, point x_g may have to be defined by the left and right limits of the coordinate, respectively, to express the discontinuity here explicitly, that means $x_g^l = f^{-1}(x_B) = f^{-2}(x_F)$ and $x_g^r = f^{-1}(x_C) = f^{-2}(x_A)$. As shown in Fig. 1, point x_g divides the exit into two equal parts. If an iteration out of the channel falls in the left half of the exit (the clean part in Fig. 1), it visits segment CD only once, and will then be reinjected into the farthest end of the channel, between point x_L and F. While if it falls in the right half (the region in Fig. 1 covered by thin oblique solid lines), it visits CD twice, and will then be reinjected into the nearest end of the channel, between point E and x_R. After a collision between a periodic orbit and x_g, the orbit will be replaced by a new attractor [17,18]. That means such a collision is one of the boundary conditions of the phase-locked plateaus in the devil's staircase. Of course, the collision of a periodic orbit with the gap between points D and E also determines the boundary conditions, as discussed in Sec. V. Therefore, with ϵ changing so that a periodic orbit moves, there can be at least the following four modes of collision between the orbit and the discontinuous points which confine a phase-locked plateau.

(1) In an iterated trajectory, if the iteration out of the channel always falls on the left part of the exit, the orbit collides with point E at ϵ_R, and collides with point x_g^l at ϵ_L.

(2) If the iteration out of the channel always falls in the right part of the exit, the orbit collides with point D at ϵ_L, and collides with point x_g^r at ϵ_R.

(3) If the iteration out of the channel can fall in either the left or right parts of the exit, there can be two modes of the collision: (a) the orbit collides with point x_g^l at ϵ_L and collides with point x_g^r at ϵ_R, and (b) the orbit collides with point D at ϵ_L and collides with point E at ϵ_R.

As will be discussed in Sec. III, modes (1) and (2) induce the two most important sequences of the phase-locked plateaus, while mode (3) induces the other sequences.

Before our discussion on the staircase of the phase-locked plateaus, we have to define the winding number of an iterated trajectory. For a circle map, the traditional definition of the winding number is

$$R=\lim_{N\to\infty}\frac{f^{(N)}(x_0)-x_0}{N}=\frac{p+q}{n+m+2p+3q}, \tag{2}$$

where p is the number of reinjection via the left part of the exit in an iterated trajectory, and q is that via the right part of the exit. $n=\Sigma_{i=1}{}^{p}n_i$, $m=\Sigma_{j=1}{}^{q}m_j$, where n_i is the iteration number inside the channel after the ith reinjection via the left part of the exit, and m_j is that after the jth reinjection via the right part of the exit. By this definition, R is the ratio that each iteration crosses on the average when the number of iteration $N\to\infty$. However, we prefer another definition which is more convenient for the expression of type-V intermittency appearing inside the staircase, and for the calculation of the Lyapunov exponents. The new definition is

$$\omega=\frac{n+m}{n+m+2p+3q}. \tag{3}$$

By this definition, the winding number is the proportion of the iteration number inside the channel to the total iteration number in the trajectory. In Sec. V, we will show that definitions (2) and (3) give similar staircase structures.

Now the expression of the Lyapunov exponent of an iterated trajectory can be easily derived as

$$\lambda(\epsilon)=\lim_{N\to\infty}\frac{1}{N}\sum_{i=0}^{N-1}\ln|f'(x_i)|=[1-\omega(\epsilon)]\ln k_1+\omega(\epsilon)\ln k_2. \tag{4}$$

Keener [34] proved analytically that the dynamics of a discontinuous circle map is dominated by periodic attractors, while chaotic attractors may appear in a mapping with an overlapping part. Here, mapping (1) has both the discontinuities and an overlapping part, and therefore we may expect both a complete phase-locking region and a chaotic region in the parameter space [4,5,8]. When ϵ is smaller than a threshold value ϵ_{c_0}, the iteration in a trajectory should visit segment EF (with a slope smaller than a unit) much more often than segments AB and CD (with the slope larger than a unit). The Lyapunov exponent should be negative in the parameter region $[0,\epsilon_{c_0}]$ [15], that is, the complete phase-locking region. In this region the winding number ω can be calculated simply in one period. For simplicity, definitions (3) and (2) will still be used. However, in definition (2), N will denote the number of iterations in one period; in definitions (3) and (2), p will be the number of reinjections via the left part of the exit in one period, q will be that via the right part of the exit in one period, n_i will be the iteration number inside the channel after ith reinjection via the left part of the exit in one period, and m_j will be that after jth reinjection via the right part of the exit in one period. These definitions will be used in all the following sections.

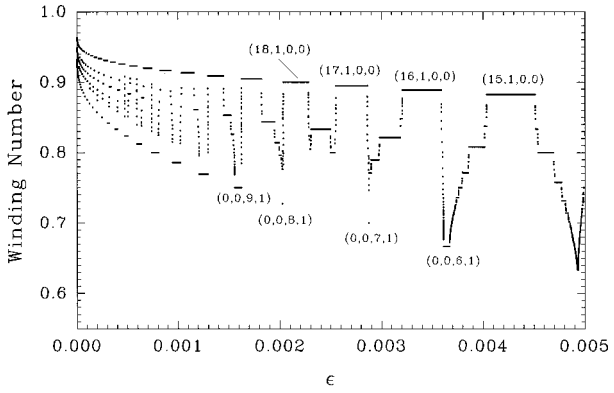

FIG. 2. The MCDS of the function $\omega(\epsilon)$ obtained numerically by definition (3). Every $\omega(\epsilon)$ value is obtained by taking an average over 5000 reinjections. The first 2000 iterations were dropped to avoid transience. Ten different initial value between -0.5 and 0.5 have been chosen for the computation. Exactly the same results were obtained, suggesting that the coexistence of periodic attractors need not be considered here.

III. THE MULTIPLE COMPLETE DEVIL'S STAIRCASE

Figure 2 shows our numerical results of the dependence of the winding number ω by definition (3), on the control parameter ϵ in the complete phase-locking region. Our computation shows that the coexistence of periodic attractors probably does not happen in this region, thus we shall not pay attention to this question. The diagram consists of many towerlike structures. After a careful study, we found that both the ascent (left) and the descent (right) branches of each tower are CCDS's. In the whole staircase, which is composed of many CCDS's and therefore is addressed as a multiple complete devil's staircase (MCDS), the dependence of ω on ϵ has lost monotonicity.

According to definition (3), one can denote each plateau by four characters, (n, p, m, and q). Between them, p and q are most important, and signify a significant feature of the periodic orbit. The feature is the number of the iteration going through the left or right parts of the exit of the channel in one period. One will see that the ratio $p:q$ determines the main sequences in the MCDS.

If $p:q=1:0$, the iteration escapes from the channel only via the left part of the exit. The number of iterations inside the channel via the right part of the exit, m, naturally equals zero. The winding number of the plateaus belonging this sequence can be written as $\omega=n/(n+2)$. In this situation the collision between the periodic orbit and the discontinuous points thus can only choose the first mode mentioned in Sec. II. In this, the orbit collides with point E at ϵ_R, and x_g^l at ϵ_L. The system is locked in an (n,1,0,0) plateau in $[\epsilon_L,\epsilon_R]$. In both cases, if $\epsilon>\epsilon_R$ or $\epsilon<\epsilon_L$, the escaping iteration will enter the right part of the exit.

If $p:q=0:1$, the iteration escapes from the channel only through the right part of the exit. Then number n equals zero, and m becomes the only varying index. The winding number of the plateaus in this sequence can be written as $\omega=m/(m+3)$. The collision condition between the periodic orbit and the discontinuous points thus can only choose the second mode mentioned in Sec. II. In this, the periodic orbit collides with point D at ϵ_L, and it collides with x_g^r at ϵ_R. The system is locked in a (0,0,m,1) plateau in $[\epsilon_L,\epsilon_R]$. In both cases, if

$\epsilon > \epsilon_R$ or $\epsilon < \epsilon_L$, the escaping iteration will enter the left part of the exit.

As can be seen in Fig. 1, the iteration escaping through the left part of the exit will be reinjected into the part of the channel farthest from the exit, and the iteration escaping through the right part of the exit will be reinjected into the part of the channel nearest to the exit. Therefore, the winding number of a 1:0 plateau should be much larger than that of its neighboring 0:1 plateau. The sequence of the 1:0 plateaus and that of the 0:1 plateaus are separated by a large vertical distance in the ω-ϵ plane. Considering the fact that many $p{:}q$ ($p>0$ *and* $q>0$) plateaus should appear between neighbor 1:0 and 0:1 plateaus; there should be tower structures in the ω-ϵ plane. In this plane, $(n,1,0,0)$ denotes the sequence of the ''top'' plateaus in the towers, and $(0,0,m,1)$ denotes the sequence of the ''bottom'' plateaus in the towers as shown in Fig. 2.

Now we shall derive mathematical expressions of the stability borders of the phase-locked plateaus belonging to different $p{:}q$ sequences in the MCDS. The derivation and the expressions are quite long and boring; therefore, only some main results are presented here. A reader who would like to know additional can find more details in the Appendix.

(a) $p{:}q=1{:}0$ sequence: For this sequence, the periodic condition requires

$$f_2^{(n)} f_{11} f_{12}(x) = x. \tag{5}$$

When $\epsilon \to 0$, we define collision functions as

$$L_n^-(x) = f_2^{(n)} f_{11} f_{12}(x), \quad x < \epsilon/2 \quad \text{and} \quad x \to \epsilon/2 \tag{6}$$

and

$$L_n^+(x) = f_2^{(n-1)} f_{11} f_{12} f_2(x), \quad x > \epsilon \quad \text{and} \quad x \to \epsilon. \tag{7}$$

Here L_n^- represents a periodic point which is about to collide with the discontinuous point x_g^l, while L_n^+ represents a periodic point which is about to collide with the discontinuous point E. Substituting Eq. (1) into Eqs. (6) and (7), one obtains

$$L_n^-(x) = 2xG(n) - \epsilon G(n) - \epsilon Q(n) + P(n) \tag{8}$$

and

$$L_n^+(x) = 2(x-\epsilon)G(n) - \epsilon G(n-1) - \epsilon Q(n-1) + P(n-1), \tag{9}$$

where

$$G(n) = \tfrac{1}{2} k_1^2 k_2^n, \quad Q(n) = \frac{1-k_2^n}{1-k_2} k_2, \quad P(n) = \tfrac{1}{2} k_2^n.$$

The collision conditions are $L_n^-(\epsilon_L/2) = \epsilon_L/2$, and $L_n^+(\epsilon_R) = \epsilon_R$. We can obtain the expression of the two end points of a plateau $(n,1,0,0)$ as

$$\epsilon_L(n,1,0,0) = \frac{P(n)}{\frac{1}{2} + Q(n)}, \tag{10}$$

$$\epsilon_R(n,1,0,0) = \frac{P(n-1)}{1 + Q(n-1) + G(n-1)}. \tag{11}$$

(b) $p{:}q=0{:}1$ sequence: Similarly, we can define collision functions as

$$R_m^-(x) = f_2^{(m)} f_{11} f_{12}^{(2)}(x), \quad x < \epsilon \quad \text{and} \quad x \to \epsilon \tag{12}$$

and

$$R_m^+(x) = f_2^{(m-1)} f_{11} f_{12}^{(2)} f_2(x), \quad x > \epsilon/2 \quad \text{and} \quad x \to \epsilon/2, \tag{13}$$

where R_m^+ represents a periodic point which is about to collide with the discontinuous point x_g^r, while R_m^- represents a periodic point which is about to collide with the discontinuous point D. Substituting Eq. (1) into Eqs. (12) and (13), one obtains

$$R_m^-(x) = 2xT(m) - \epsilon T(m) - \epsilon S(m) + O(m) \tag{14}$$

and

$$R_m^+(x) = 2(x-\epsilon)T(m) - \epsilon T(m-1) - \epsilon S(m-1) + O(m-1), \tag{15}$$

where

$$T(m) = \tfrac{1}{2} k_1^3 k_2^m, \quad S(m) = \frac{k_1^2 k_2^m}{2(1+k_1)} + \frac{1-k_2^m}{1-k_2} k_2,$$

$$O(m) = \frac{1 + k_1 - k_1^2}{2(1+k_1)} k_2^m.$$

Thus the two end points of a plateau $(0,0,m,1)$ in this sequence can be obtained by the collision conditions $R_m^-(\epsilon_L) = \epsilon_L$ and $R_m^+(\epsilon_R/2) = \epsilon_R/2$, as

$$\epsilon_L(0,0,m,1) = \frac{O(m)}{1 + S(m) - T(m)}, \tag{16}$$

$$\epsilon_R(0,0,m,1) = \frac{O(m)}{\frac{1}{2} + S(m)}. \tag{17}$$

(c) $p{:}q=1{:}1$ sequence: According to definition (3), a plateau in this sequence has a winding number $\omega = (n+m)/(n+m+2+3)$. By the ''Farey tree rule'' stated in Sec. I, which still works in either the ascent or the descent branch of a tower, a 1:1 plateau should be the largest plateau between the neighboring top and bottom plateaus. We also address them by ''middle plateaus.''

Unlike the two situations discussed above, in this case the iteration escapes from the channel one time via the right part of the exit, and one time via the left part alternatively. Therefore there can be two modes of the collision between the periodic orbit and the discontinuous points, as mentioned in Sec. II. We found that the ascent or the descent branch of a tower shown in Fig. 2 has different choices of mode.

(i) The ascent branch: In this branch the plateaus choose mode (a) in the third case stated in Sec. II. That is, iteration in the periodic orbit via the left half of the exit collides with x_g^l at ϵ_L, while the iteration via the right half of the exit collides with x_g^r at ϵ_R. Therefore the collision function can be defined as

$$F_a^-(x)=R_m^-L_n^-(x), \quad x<\epsilon/2 \quad \text{and} \quad x\to\epsilon/2, \tag{18}$$

and

$$F_a^+(x)=L_n^-R_m^-(x), \quad x>\epsilon/2 \quad \text{and} \quad x\to\epsilon/2. \tag{19}$$

Similarly we can obtain the expressions

$$\epsilon_L(n,1,m,1)=\frac{O(m)+2T(m)P(n)}{\frac{1}{2}+S(m)+T(m)+2T(m)Q(n)}, \tag{20}$$

$$\epsilon_R(n,1,m,1)=\frac{P(n)+2G(n)O(m)}{\frac{1}{2}+Q(n)+G(n)+2G(n)S(m)}. \tag{21}$$

(ii) The descent branch: In this branch the plateaus choose mode (b) in the third case stated in Sec. II. That is, iteration in the periodic orbit via the right half of the exit collides with point D at ϵ_L, while the iteration via the left half of the exit collides with point E at ϵ_R. Therefore we can have the similar expressions

$$F_d^-(x)=L_n^-R_m^-(x), \quad x<\epsilon \quad \text{and} \quad x\to\epsilon, \tag{22}$$

$$F_d^+(x)=R_m^+L_n^+(x), \quad x>\epsilon \quad \text{and} \quad x\to\epsilon \tag{23}$$

and

$$\epsilon_L(n,1,m,1)=\frac{P(n)+2G(n)O(m)}{\frac{1}{2}+Q(n)+G(n)+2G(n)[S(m)-T(m)]}, \tag{24}$$

$$\epsilon_R(n,1,m,1)=\frac{O(m-1)+2T(m)P(n-1)}{1+S(m-1)+T(m-1)+2T(m)[1+G(n-1)+Q(n-1)]}. \tag{25}$$

(d) $p{:}q$ ($p>1$ *and* $q>1$) sequences of the phase-locked plateaus (the plateaus in both the ascent and the descent branches of the towers are shown in Fig. 2, which form many sequences between 1:0, 1:1, and 0:1).

In this general case, there can be again two modes of the collision between the periodic orbit and the discontinuous points, which is the same as in the situation where $p{:}q=1{:}1$. A reasonable conclusion is that the collision function can still be expressed by a combination of R_m^-, R_m^+, L_n^-, and L_n^+, but the form will be much more complicated. We shall present only the mathematical forms of the collision functions and the collision conditions in the Appendix. Explicit expressions of $\epsilon_L(n,p,m,q)$ and $\epsilon_R(n,p,m,q)$ are too long and too complicated to present. In practice, we would prefer to use a numerical way to obtain the data of $\epsilon_L(n,p,m,q)$ and $\epsilon_R(n,p,m,q)$ by a substitution of mapping (1) and the collision conditions to the collision functions. We have compared all the analytical results of $\epsilon_L(n,p,m,q)$ and $\epsilon_R(n,p,m,q)$ with the numerically obtained positions of plateaus shown in Fig. 2, and seen very good agreement.

It is now clear that the MCDS has neither monotonicity nor exact self-similarity. This means that winding numbers may increase or decrease in different parts of a MCDS, and a magnification of a small part of a MCDS may not resemble itself. Also, the distribution rule of the lengths of the phase-locked plateaus in a MCDS cannot be described by a Farey tree. For example, as can be seen in Fig. 2, the largest plateau between two plateaus, M_1/s_1 and M_2/s_2, often is a plateau belonging to the ''top'' sequence instead of $(M_1+M_2)/(s_1+s_2)$ if plateaus M_1/s_1 and M_2/s_2 are not in same branch of a tower. That does not obey the ''Farey tree rule'' in a CCDS.

IV. TYPE-V INTERMITTENCY INSIDE A MCDS

From Eq. (4), one knows that the Lyapunov exponent function of the driving parameter, $\lambda(\epsilon)$, should show a similar MCDS in the λ-ϵ plane. Figure 3 shows this MCDS. It has similar tower structures, but the 1:0 sequence is in the

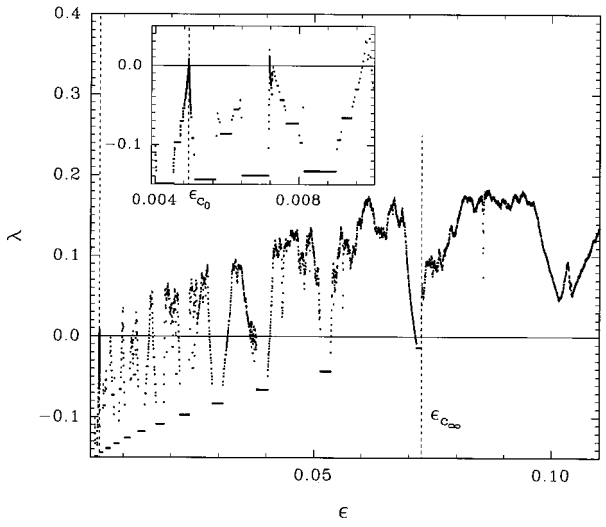

FIG. 3. The Lyapunov exponent spectrum to show the transition of the $p{:}q$ sequences to chaos. The inset is the enlargement of the part within the parameter range [0.0040,0.0101]. The two vertical dashed lines indicate the first and the last thresholds, where the 0:1 or the 1:0 sequence turns to chaos. Every $\lambda(\epsilon)$ value is obtained with Eq. (4) by taking an average over 5000 reinjections and ten initial numbers. The first 2000 iterations were dropped to avoid transience.

lowest position there. Also, the range of the driving parameter in Fig. 3 is much wider than that in Fig. 2, to show how the different $p:q$ sequences turn to chaos via type-V intermittencies in different ϵ values. It is interesting to study these critical values of ϵ and the scaling properties of these type-V intermittency inside the MCDS. We shall present the results in this section.

In this study, we prefer to estimate these critical values by calculating the ϵ values at which the aforementioned sequences stop. Here ''stop'' means that all the plateaus of a sequence positioned over the criticality will lose stability, and the system shows a chaotic motion there. As examples, Fig. 3 shows ϵ_{c_∞}, where the 1:0 sequence stops, and ϵ_{c_0}, where the 0:1 sequence stops. One can see that these two ϵ values are very near to the criticalities of the two $p:q$ sequences. If comparing ω and λ values of different plateaus belonging to the same tower, one knows from Eq. (4) that the plateau with the smaller winding number has the larger Lyapunov exponent. Hence the 0:1 sequence loses its stability first, and the 1:0 sequence turns to chaos last, as shown clearly in Fig. 3.

Now we estimate the value of ϵ_{c_0} at which the 0:1 sequence stops. The stability condition of a periodic attractor in this sequence is

$$k_1^3 k_2^m \leqslant 1. \tag{26}$$

Thus, at $\epsilon=\epsilon_{c_0}$, the critical stability condition

$$k_1^3 k_2^{m_c} = 1 \tag{27}$$

should be satisfied, where m_c denotes the critical value of m. Thus we have

$$m_c = -3\ln k_1 / \ln k_2 = 5.451\,178\,47\ldots\ . \tag{28}$$

For a rough estimate, we take the nearest integer value, which is smaller than m_c. That is $m_c = 5$. Substituting this m_c value into Eq. (17), one can obtain the lower limit of ϵ_{c_0}, i.e., $\epsilon_{c_0} > 0.004\,910\,18$.

The critical value ϵ_{c_∞}, where the 1:0 sequence turns to chaos, can be estimated in a similar way. At $\epsilon=\epsilon_{c_\infty}$, the critical stability condition

$$k_1^2 k_2^{n_c} = 1 \tag{29}$$

should be satisfied. Thus we have

$$n_c = -2\ln k_1 / \ln k_2 = 3.634\,118\,9\ldots\ . \tag{30}$$

For a rough estimate, we take the nearest integer value which is smaller than n_c. That is $n_c = 3$. Substituting this n_c value into Eq. (11), one can obtain the lower limit of ϵ_{c_∞}, i.e., $\epsilon_{c_\infty} > 0.010\,265\,8$.

Similarly we can obtain the estimates of other critical values between ϵ_{c_0} and ϵ_{c_∞} at which other sequences turn to chaos. These values are in a tolerable agreement with the numerical results. For example, the numerical critical values of ϵ_{c_0} and ϵ_{c_∞} are 0.004 919 70 and 0.027 572 9, respectively. They are near to our estimates.

As shown in Fig. 3, in the parameter region where $\epsilon < \epsilon_{c_0}$, periodic attractors dominate the system's dynamics. We say that this is a ''complete phase-locking'' region. In the parameter region where $\epsilon > \epsilon_{c_\infty}$, there can be only chaotic attractors. While in the region where $\epsilon_{c_0} < \epsilon < \epsilon_{c_\infty}$, periodic and chaotic attractors appear alternately. Many sequences addressed by $p:q$ ($p>0$ and $q>0$) turn to chaos via a type-V intermittency there. Therefore type-V intermittency appears frequently in the MCDS in this region. This is another characteristic of the MCDS.

Now we shall derive the main scaling properties of the so-called ''type-V intermittency inside a MCDS.'' The properties studied here are the scaling of the average laminar lengths and the scaling of the Lyapunov exponent.

For the 1:0 sequence, when $\epsilon \to 0$ and $n \to \infty$, Eqs. (10) and (11) show the same dependence of the winding number ω on ϵ as

$$\omega \simeq 1 - 2\frac{\ln k_2}{\ln \epsilon}. \tag{31}$$

Similarly, for the 0:1 sequence, when $\epsilon \to 0$ and $n \to \infty$, Eqs. (16) and (17) show the same dependence of the winding number ω on ϵ,

$$\omega \simeq 1 - 3\frac{\ln k_2}{\ln \epsilon}. \tag{32}$$

For the 1:1 sequence, when $\epsilon \to 0$ and $n \to \infty$, Eqs. (20), (21), (24), and (25) show the same dependence of the winding number as the geometrical average of Eqs. (31) and (32),

$$\omega \simeq 1 - \frac{2+3}{2}\,\frac{\ln k_2}{\ln \epsilon}. \tag{33}$$

Therefore we would expect a form of the dependence of the winding number for $p:q$ sequences, the general case, as

$$\omega \simeq 1 - \frac{2p+3q}{p+q}\,\frac{\ln k_2}{\ln \epsilon}. \tag{34}$$

Thus the Lyapunov exponent scales as

$$\lambda \simeq \ln k_2 - \frac{E(p,q)}{\ln \epsilon}, \tag{35}$$

where

$$E(p,q) = \frac{2p+3q}{p+q}\ln k_2 (\ln k_2 - \ln k_1).$$

In order to verify the analytical conclusion expressed by Eq. (35), the results of the dependence of the Lyapunov exponent on ϵ obtained by both Eq. (35) and the direct numerical computation by Eq. (4) have been compared, as shown in Fig. 4. For simplicity, only the numerical results of the Lyapunov exponent plateaus for three sequences, called 1:0, 1:1, and 0:1, are shown in the figure from bottom to top. The corresponding solid lines are drawn by Eq. (35). The dashed horizontal line, denoted by $\lambda = \ln k_2$ in the figure, indicates the limit value of the Lyapunov exponent for all the se-

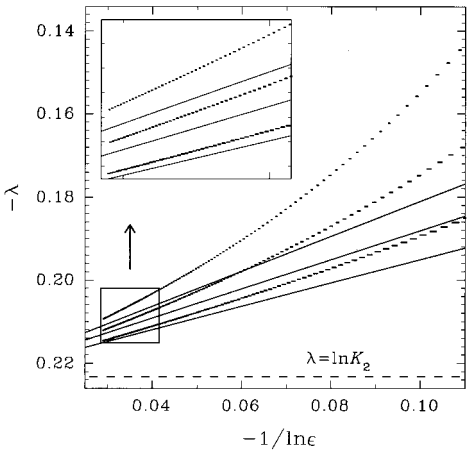

FIG. 4. The scaling properties of the Lyapunov exponents of three sequences in the range $0.000\,000\,1<\epsilon<0.005$. From bottom to top, the computed plateaus belong to 1:0, 1:1, and 0:1 sequences in turn. Every λ value is obtained with Eq. (4) by taking an average over 5000 reinjections and ten initial numbers. The first 2000 iterations were dropped to avoid transience. The three solid lines show the analytical results of Eq. (35).

quences when $\epsilon=0$. One can see that the agreement is excellent. A similar comparison has also been made for some of the $p:q$ sequences. The good agreement makes sure that Eq. (35) is correct.

Finally, the dependence of the average laminar lengths on ϵ can be obtained easily as

$$\langle l\rangle=\frac{n+m}{p+q}\simeq\frac{\ln\epsilon}{\ln k_2}-\frac{2p+3q}{p+q}. \tag{36}$$

We may need to point out that the function $\langle l\rangle(\epsilon)$ is also a MCDS as the function $\omega(\epsilon)$ and $\lambda(\epsilon)$. Now our study in this section shows that the scaling laws of type-V intermittency inside a MCDS are still reasonably consistent with the general conclusion reported in Refs. [10,11,15].

V. DISCUSSION

In this section a discussion on some further questions will be presented. The first question may be the following: Is there still a MCDS in this system if a winding number is defined in the traditional way as expressed by Eq. (2)? In other words, is it possible that the MCDS reported in this paper only comes from the special definition of the winding number as expressed by Eq. (3)?

From the discussion in the above three sections, one can already obtain the conclusion that the MCDS in this system is induced by the complicated modes of a collision between a periodic orbit and discontinuous points. In the system studied in Ref. [15], there is only one of these modes: the collision conditions of a periodic orbit with only two discontinuous points confine all the phase-locked plateaus. This simple mechanism generates a CCDS. In the case when more than two discontinuous points exist, and all of them can show influences on the periodic condition, the different modes of the collision will induce different kinds of CCDS's. These CCDS's organize a complicated staircase due to the cross-correlation between the different modes. Therefore the

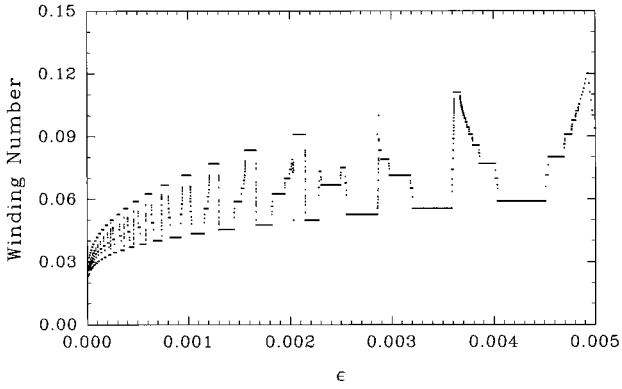

FIG. 5. The MCDS of the function $\omega(\epsilon)$ obtained numerically by definition (2). Every $\omega(\epsilon)$ values is obtained by taking an average over 5000 reinjections. The first 2000 iterations were dropped to avoid transience. Ten different initial value, x_0, between -0.5 and 0.5, have been chosen for the computation. The results are same. This figure shows that definitions (2) and (3) induce similar MCDS's.

MCDS is a property of a ''multigap'' map. It exists no matter what kind of a reasonable definition for a winding number is suggested.

In order to verify this conclusion, we computed the function $\omega(\epsilon)$ by definition (2). The results are shown in Fig. 5. One can see that the MCDS in Fig. 5 is upside down, but still has almost the same form as that in Fig. 2.

The next question is the following: Is it possible that the MCDS can be observed in a everywhere-differentiable mapping? As is well known, in a one-dimensional map, $f(x)$, which is everywhere differentiable, the critical stability condition of a period-p attractor can be expressed as

$$\left|\frac{df^p(x)}{dx}\right|=1. \tag{37}$$

We argue that this condition can be viewed as a kind of ''mode'' for confining phase-locked plateaus. There can be only this mode in this system. It is not strange, then, to see a CCDS in such a map, just like what was reported in Ref. [25–33].

The situation becomes different in a one-dimensional map which has gaps. In addition to what is expressed by Eq. (37), the modes for determining both end points of a phase-locked plateau can be also the condition of the collision between the periodic orbit and the discontinuous points as discussed in this paper. These modes may induce a MCDS. In the point of view of symbolic dynamics, a mapping with gaps needs more symbols to be described. A scientist studying symbolic dynamics may express this idea as follows: A discontinuous map has higher dimensions than an everywhere-differentiable map does, which is why it can show more complicated behaviors.

Considering the discussion above, we argue that is a possibility to observe a kind of MCDS in a high-dimensional everywhere-differentiable map. To our knowledge, no such phenomenon has been discovered yet. We expect to see such an observation.

The last question is the following: Can we compare the $p:q$ sequences in this investigation with the famous ''period-

adding sequences'' [35]? As suggested by Kaneko, a period-adding sequence is composed of phase-locked plateaus with the winding number $(un+s)/(vn+r)$ chosen among the plateaus in a CCDS located between two plateaus with the winding numbers u/v and s/r (u,v,s,r, and n are integers). The reason for this choice is that it is feasible to observe this sequence since it has a large stable region, and that it reveals the global property of lockings through various scalings [35]. In an experimental observation, when varying the driven parameter so that n develops, one often sees that the system is locked onto a sequence of periodic motion, and the difference between the neighboring locking periods is either u or v. In the MCDS, in each $p:q$ sequence, n and m increase alternatively when ϵ decreases, so that the difference between the periods of the neighboring plateaus is also a constant; therefore we suggest calling them period-adding sequences. Of course they have some special features if compared with those in a CCDS. First, in the situation stated by Kaneko, each sequence occupies a different part of the parameter axis. In the MCDS the phase-locked plateaus of each sequence are distributed in the whole complete phase-locking region, which is approximately the region between $\epsilon=0$ and 0.005 in this investigation. Second, the period-adding sequences in the MCDS are located in different positions along the vertical, i.e., the ω, direction. The sequence in highest position is the 1:0 sequence with the winding numbers $n/(n+2)$, while the 0:1 sequence with the winding numbers $m/(m+3)$ has the lowest position. There are many of $p:q$ period-adding sequences located between the sequences 1:0 and 0:1. The plateaus belonging to them are distributed in a special way, so that the plateaus positioned between every pair of the neighboring 1:0 and 0:1 plateaus form a CCDS. Among these $p:q$ period-adding sequences the sequence 1:1 with the winding numbers $(n+m)/(n+m+2+3)$ is composed of the largest plateaus. In this way, a MCDS may be described as a queue of period-adding sequences on the ϵ-ω plane. Last, we have proved that the scaling behaviors of the period-adding sequences in the MCDS are qualitatively different from those in a CCDS. The calculation and the results about these scaling laws will be presented elsewhere.

ACKNOWLEDGMENTS

This work was supported by the Chinese National Science Foundation under Grant No. 19575037. All of the authors want to express their gratitude to Professor E. J. Ding for his very important suggestions and calculations.

APPENDIX

For the general $p:q$ ($p>1$ *and* $q>1$) sequences we have the following expressions.

(i) The ascent branch: As defined in Eq. (3), one has

$$n=n_1+n_2+\cdots+n_p, \quad n_i=[in/p]-[(i-1)n/p]$$

and

$$m=m_1+m_2+\cdots+m_q, \quad m_j=[jm/q]-[(j-1)m/q]$$

where $i=1,2,\ldots,p$, $j=1,2,\ldots,q$, and [ ] represents ''the integer part.'' If $p<q$, the collision functions can be written as

$$F_a^-(x)=\left(\prod_{l=1}^{[q/p]} R^-_{m_{lp}}\right)\left(\prod_{i=0}^{|D_{q,p}|-1}\ \prod_{j=0}^{B_i(q,p,0)} L^-_{n_{\nu(i,j,q,p,0)}}\ \prod_{t=0}^{H_{i,j}(q,p,0)} R^-_{m_{\nu(i,j,q,p,0)+tp}}\right)L^-_{n_p}(x), \tag{A1}$$

$$x<\epsilon/2 \quad \text{and} \quad x\to\epsilon/2,$$

$$F_a^+(x)=\left(\prod_{l=1}^{[q/p]} R^-_{m_{1+lp}}\right)\left(\prod_{i=0}^{|D_{q,p}|-1}\ \prod_{j=0}^{B_i(q,p,1)} L^-_{n_{\nu(i,j,q,p,1)}}\ \prod_{t=0}^{H_{i,j}(q,p,1)} R^-_{m_{\nu(i,j,q,p,1)+tp}}\right)L^-_{n_1}R^-_{m_1}(x), \tag{A2}$$

$$x>\epsilon/2 \quad \text{and} \quad x\to\epsilon/2.$$

If $p\geqslant q$, the collision functions can be written as

$$F_a^-(x)=\left[\prod_{i=0}^{|D_{p,q}|-1}\ \prod_{j=0}^{B_i^*(p,q,1)}\left(\prod_{t=H^*_{i,j}(p,q,1)}^{0} L^-_{n_{\nu^*(i,j,p,q,1)+tp}}\right)R^-_{m_{\nu^*(i,j,p,q,1)}}\right]\left(\prod_{l=[p/q]}^{1} L^-_{n_{lq}}\right)R^-_{m_q}L^-_{n_p}(x), \tag{A3}$$

$$x<\epsilon/2 \quad \text{and} \quad x\to\epsilon/2,$$

$$F_a^+(x)=\left[\prod_{i=0}^{|D_{p,q}|-1}\ \prod_{j=0}^{B_i^*(p,q,0)}\left(\prod_{t=H^*_{i,j}(p,q,0)}^{0} L^-_{n_{\nu^*(i,j,p,q,0)+tp}}\right)R^-_{m_{\nu^*(i,j,p,q,0)}}\right]\left(\prod_{l=[p/q]}^{0} L^-_{n_{1+lq}}\right)R^-_{m_1}(x), \tag{A4}$$

$$x>\epsilon/2 \quad \text{and} \quad x\to\epsilon/2.$$

The collision conditions are $F_a^-(\epsilon_L/2)=\epsilon_L/2$ and $F_a^+(\epsilon_R/2)=\epsilon_R/2$.

(ii) The descent branch: If $p\leqslant q$, the collision functions can be written as

$$F_d^-(x)=\left[\prod_{i=0}^{|D_{q,p}|-1}\prod_{j=0}^{B_i^*(q,p,1)}\left(\prod_{t=H_{i,j}^*(q,p,1)}^{0}R^-_{m_{\nu^*(i,j,q,p,1)+tp}}\right)L^-_{n_{\nu^*(i,j,p,q,1)}}\right]\left(\prod_{l=[q/p]}^{1}R^-_{m_{lp}}\right)L^-_{n_p}R^-_{m_q}(x), \tag{A5}$$

$$x<\epsilon \quad \text{and} \quad x\to\epsilon,$$

$$F_d^+(x)=\left[\prod_{i=0}^{|D_{q,p}|-1}\prod_{j=0}^{B_i^*(q,p,0)}\left(\prod_{t=H_{i,j}^*(q,p,0)}^{0}R^+_{m_{\nu^*(i,j,q,p,0)+tp}}\right)L^+_{n_{\nu^*(i,j,q,p,0)}}\right]\left(\prod_{l=[q/p]}^{0}R^+_{m_{1+lp}}\right)L^+_{n_1}(x), \tag{A6}$$

$$x>\epsilon \quad \text{and} \quad x\to\epsilon.$$

If $p>q$, the collision functions can be written as

$$F_d^-(x)=\left(\prod_{l=1}^{[p/q]}L^-_{n_{lq}}\right)\left(\prod_{i=0}^{|D_{p,q}|-1}\prod_{j=0}^{B_i(p,q,0)}R^-_{m_{\nu(i,j,p,q,0)}}\prod_{t=0}^{H_{i,j}(p,q,0)}L^-_{n_{\nu(i,j,p,q,0)+tq}}\right)R^-_{m_p}(x), \tag{A7}$$

$$x<\epsilon \quad \text{and} \quad x\to\epsilon,$$

$$F_d^+(x)=\left(\prod_{l=1}^{[p/q]}L^+_{n_{1+lp}}\right)\left(\prod_{i=0}^{|D_{p,q}|-1}\prod_{j=0}^{B_i(p,q,1)}R^+_{m_{\nu(i,j,p,q,1)}}\prod_{t=0}^{H_{i,j}(p,q,1)}L^+_{n_{\nu(i,j,p,q,1)+tq}}\right)R^+_{m_1}L^+_{n_1}(x), \tag{A8}$$

$$x>\epsilon \quad \text{and} \quad x\to\epsilon.$$

The collision conditions are $F_d^-(\epsilon_L)=\epsilon_L$ and $F_d^+(\epsilon_R)=\epsilon_R$. The functions D, B, ν, H, B^*, ν^*, and H^* are defined as

$$D_{\sigma,\tau}=\begin{cases}A_{\sigma,\tau}, & A_{\sigma,\tau}\leqslant[\tau/2]\\ A_{\sigma,\tau}-\tau, & A_{\sigma,\tau}>[\tau/2],\end{cases}$$

where $A_{\sigma,\tau}=\sigma-\tau[\sigma/\tau]$;

$$\nu(i,j,\sigma,\tau,\delta)=\mu(i,j,\sigma,\tau,\delta)-jD_{\sigma,\tau},$$

where

$$\mu(i,\sigma,\tau,\delta)=\begin{cases}\tau-A_{\sigma,\tau}+\delta, & i=0\\ \tau-A_{\sigma,\tau}+\delta+i\ \mathrm{sgn}(D_{\sigma,\tau}), & i\neq 0,\ (\tau-1)-A_{\sigma,\tau}[(\tau-1)/A_{\sigma,\tau}]=0\\ \tau-A_{\sigma,\tau}+\delta+(|D_{\sigma,\tau}|-i)\ \mathrm{sgn}(D_{\sigma,\tau}), & i\neq 0,\ (\tau-1)-A_{\sigma,\tau}[(\tau-1)/A_{\sigma,\tau}]\neq 0,\end{cases}$$

$$B_i(\sigma,\tau,\delta)=\begin{cases}[\mu(i,\sigma,\tau,\delta)+1-\tau+\delta]/D_{\sigma,\tau}, & D_{\sigma,\tau}<0\\ (\mu(i,\sigma,\tau,\delta)-1-\delta]/D_{\sigma,\tau}, & D_{\sigma,\tau}\geqslant 0;\end{cases}$$

$$H_{i,j}(\sigma,\tau,\delta)=\begin{cases}E, & \nu(i,j,\sigma,\tau,\delta)\leqslant A_{\sigma,\tau}\\ E-1, & \nu(i,j,\sigma,\tau,\delta)>A_{\sigma,\tau},\end{cases}$$

where $E=[\sigma/\tau]$; and

$$\nu^*(i,j,\sigma,\tau,\delta)=\mu^*(i,j,\sigma,\tau,\delta)+jD_{\sigma,\tau},$$

where

$$\mu^*(i,\sigma,\tau,\delta)=\begin{cases} A_{\sigma,\tau}+1-\delta, & i=0 \\ A_{\sigma,\tau}+1-\delta+i\ \mathrm{sgn}(D_{\sigma,\tau}), & i\neq 0,\ (\tau-1)-A_{\sigma,\tau}[(\tau-1)/A_{\sigma,\tau}]=0 \\ A_{\sigma,\tau}+1-\delta+(|D_{\sigma,\tau}|-i)\ \mathrm{sgn}(D_{\sigma,\tau}), & i\neq 0,\ (\tau-1)-A_{\sigma,\tau}[(\tau-1)/A_{\sigma,\tau}]\neq 0, \end{cases}$$

$$B_i^*(\sigma,\tau,\delta)=\begin{cases} [2-\delta-\mu^*(i,\sigma,\tau,\delta)]/D_{\sigma,\tau}, & D_{\sigma,\tau}<0 \\ (\tau-\delta-\mu^*(i,\sigma,\tau,\delta)]/D_{\sigma,\tau}, & D_{\sigma,\tau}\geqslant 0, \end{cases}$$

$$H_{i,j}^*(\sigma,\tau,\delta)=\begin{cases} E, & \nu^*(i,j,\sigma,\tau,\delta)\leqslant A_{\sigma,\tau}-\delta \\ E-1, & \nu^*(i,j,\sigma,\tau,\delta)>A_{\sigma,\tau}-\delta. \end{cases}$$

[1] L. Glass and J. Belair, Lect. Notes Biomath. **66**, 232 (1986).
[2] L. Glass, Chaos **1**, 13 (1991).
[3] P. Alstrøm and M.T. Levinsen, Phys. Lett. A **128**, 187 (1988).
[4] B. Christiansen, P. Alstrøm, and M.T. Levinsen, Phys. Rev. A **42**, 1891 (1990).
[5] B. Christiansen, D.-R. He, S. Habip, M. Bauer, U. Krueger, and W. Martienssen, Phys. Rev. A **45**, 8450 (1992).
[6] D.-R. He, B.-H. Wang, M. Bauer, S. Habip, U. Krueger, W. Martienssen, and B. Christiansen, Physica D **79**, 335 (1994).
[7] D.-R. He, E.J. Ding, M. Bauer, S. Habip, U. Krueger, W. Martienssen, and B. Christiansen, Europhys. Lett. **26**, 165 (1994).
[8] S. Guan, B.-H. Wang, D.-k. Wang, and D.-R. He, Phys. Rev. E **52**, 453 (1995).
[9] S.-X. Qu, B. Christiansen, and D.-R. He, Phys. Lett. A **201**, 413 (1995).
[10] M. Bauer, S. Habip, D.-R. He, and W. Martienssen, Phys. Rev. Lett. **68**, 1625 (1992).
[11] D.-R. He, M. Bauer, S. Habip, U. Krueger, W. Martienssen, B. Christiansen, and B.-H. Wang, Phys. Lett. A **171**, 61 (1992).
[12] F. Ji and D.-R. He, Phys. Lett. A **177**, 125 (1993).
[13] J. Fan, F. Ji, S. Guan, B.-H. Wang, and D.-R. He, Phys. Lett. A **182**, 232 (1993).
[14] J. Fan, F. Ji, B.-H. Wang, and D.-R. He, Phys. Lett. A **191**, 139 (1994).
[15] S. Wu, E.J. Ding, and D.-R. He, Phys. Lett. A **197**, 287 (1995).
[16] H. Lamba and C. Budd, Phys. Rev. E **50**, 84 (1994).
[17] H.E. Nusse, E. Ott, and J.A. Yorke, Phys. Rev. E **49**, 1073 (1994).
[18] H.E. Nusse and J.A. Yorke, Physica D **57**, 39 (1992).
[19] H. Lamba, Physica D **82**, 117 (1995).
[20] C. Budd and F. Dux, Nonlinearity **7**, 1191 (1994).
[21] C. Budd and F. Dux, Philos. Trans. R. Soc. London, Ser. A **347**, 365 (1994).
[22] W. Chin, E. Ott, H.E. Nusse, and C. Grebogi, Phys. Lett. A **201**, 197 (1995); Phys. Rev. E **50**, 4427 (1994).
[23] C. Wunderlich, L. Moorman, and P.M. Koch, Phys. Lett. A **176**, 317 (1993).
[24] R. Richter, A. Kittel, K. Pyragas, J. Peinke, and J. Parisi, Z. Phys. B **91**, 527 (1993).
[25] P. Bak, Phys. Today **39** (12), 38 (1986).
[26] P. Bak and R. Bruinsma, Phys. Rev. Lett. **49**, 249 (1982).
[27] S. Aubry, in *Solitons and Condensed Matter Physics*, edited by A.R. Bishop and T. Schneider (Springer, Berlin, 1979), p. 264.
[28] P. Bak and J. von Boehm, Phys. Rev. B **21**, 5297 (1980); M.H. Jensen and P. Bak, *ibid.* **27**, 6853 (1983).
[29] W.-J. Yeh, D.-R. He, and Y.H. Kao, Phys. Rev. B **31**, 1359 (1985); Phys. Rev. Lett. **52**, 480 (1984).
[30] S. Martin and W. Martienssen, Phys. Rev. Lett. **56**, 1522 (1986).
[31] S.E. Brown, G. Mozurkewich, and G. Grüner, Phys. Rev. Lett. **52**, 2277 (1984).
[32] D.-R. He, D.-K. Wang, K.-J. Shi, C.-H. Yang, L.-Y. Chao, and J.Y. Zhang, Phys. Lett. A **136**, 363 (1989).
[33] M.H. Jensen, P. Bak, and T. Bohr, Phys. Rev. A **30**, 1960 (1984); **30**, 1970 (1984).
[34] J.P. Keener, Trans. Am. Math. Soc. **261**, 589 (1980).
[35] K. Kaneko, Prog. Theor. Phys. **68**, 669 (1982); **69**, 403 (1983).